Heliyon 10 (2024) e23633

Contents lists available at ScienceDirect

Heliyon

journal homepage: www.cell.com/heliyon

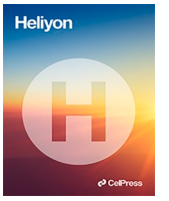

Moxibustion-mediated alleviation of synovitis in rats with rheumatoid arthritis through the regulation of NLRP3 inflammasome by modulating neutrophil extracellular traps

Miao Wang [a], Hongfang Zhao [a], Hui Zhao [a], Chenlu Huo [a], Yu Yuan [a], Yan Zhu [b,*]

[a] Anhui University of Chinese Medicine, Hefei, 230031, China
[b] The Geriatrics, The Second Affiliated Hospital of Anhui University of Chinese Medicine, Hefei, 230061, China

ARTICLE INFO

Keywords:
Moxibustion
Neutrophil extracellular traps
NLRP3 inflammasome
Rheumatoid arthritis
Synovial inflammation

ABSTRACT

Purpose: This study investigates the potential mechanism of moxibustion in the treatment of rheumatoid arthritis (RA) by regulating the neutrophil extracellular trap (NET)/NOD-like receptor family pyrin domain-containing protein 3 (NLRP3) inflammasome axis with the use of a rat model with adjuvant arthritis (AA).

Methods: Four groups, including normal control (NC), AA, moxibustion (MOX), and chlor-amidine (Cl-amidine) were created from 24 Wistar male rats (6 rats/group). After the intervention and treatment respectively, the joint swelling degree (JSD) and arthritis index (AI) were compared. The pathological changes of synovium were observed with hematoxylin and eosin staining and transmission electron microscopy. The formation of NETs in synovial tissues was detected with immunofluorescence staining. The protein expression of myeloperoxidase (MPO), neutrophil elastase (NE), citrullinated histone (Cit-H3), acyl arginine deiminase 4 (PAD-4), and NLRP3 was measured in the synovium of rat ankle joints with western blotting, and the levels of anti-cyclic citrullinated peptide antibody (CCP-Ab) and interleukin (IL)-1β were examined in rat serum with ELISA.

Results: AA modeling markedly increased JSD, AI, synovial protein expression of MPO, NE, Cit-H3, PAD-4, and NLRP3, and serum levels of CCP-Ab and IL-1β in rats ($P < 0.01$). JSD and AI, as well as the levels of MPO, NE, Cit-H3, PAD-4, NLRP3, CCP-Ab, and IL-1β, were significantly lowered in AA rats by MOX and Cl-amidine ($P < 0.01$). In addition, AA modeling caused severe pathological injury in the synovium of rats, which was annulled by MOX and Cl-amidine. The formation of NETs in synovium was substantially promoted in rats by AA modeling and was significantly reduced in AA rats after the treatment.

Conclusion: Moxibustion can markedly alleviate synovitis and repress inflammatory factor release in AA rats, which may be achieved by diminished synthesis of NETs or their constituents and the blocked formation of NLRP3 inflammasome.

* Corresponding author.
E-mail addresses: wangmiao@stu.ahtcm.edu.cn (M. Wang), zhaohongfang2019@126.com (H. Zhao), zhaohui20200302@163.com (H. Zhao), 1279223555@qq.com (C. Huo), yuanyu0524@163.com (Y. Yuan), zydzf2008@163.com (Y. Zhu).

https://doi.org/10.1016/j.heliyon.2023.e23633
Received 26 August 2023; Received in revised form 7 December 2023; Accepted 8 December 2023
Available online 13 December 2023

1. Introduction

Rheumatoid arthritis (RA) is a systemic autoimmune disease primarily characterized by the pathological change of synovial inflammation [1–3]. Unfortunately, RA is refractory with a high prevalence rate, which calls for the urgent development of efficient treatment strategies [4].

Traditional Chinese medicine therapies, particularly moxibustion, have been demonstrated to not only ameliorate joint pain and prevent bone destruction but also control immunological responses and inflammation, thus yielding great efficacy in RA treatment [5–7]. Of note, a previous study by our group revealed that moxibustion suppressed synovitis and reduced inflammatory cytokine expression in rats with adjuvant arthritis (AA) possibly by mediating NOD-like receptor family pyrin domain-containing protein 3 (NLRP3) inflammasome [8]. The upregulation of NLRP3 inflammasome, interleukin (IL)-1β, and tumor necrosis factor-α (TNF-α) levels are positively associated with disease activity. Nevertheless, molecular mechanisms underlying NLRP3 regulation in RA remain under investigation. Anti-citrullinated protein antibodies (ACPAs) are a pathogenic factor for RA, whose formation is considered a crucial process in the pathogenesis of RA [9,10]. Additionally, neutrophil extracellular traps (NETs) have been revealed to be potentially relevant to RA pathogenesis. Specifically, NETs are released through a novel form of cell death and consist of chromatin reticulation, which have the capacity of externalizing pro-inflammatory and immunostimulatory molecules, as well as various autoantigens, and activate NLRP3 inflammasome that stimulates inflammation in RA [11,12]. Therefore, it is crucial to reduce the production of NETs or the expression of their components for the prevention or mitigation of RA.

Chlor-amidine (Cl-amidine) is an orally effective PAD inhibitor that has been shown to improve disease course and clinical manifestations in a variety of disease models [13]. Due to its favorable pharmacological effects, it is now a popular compound for the study of inflammatory diseases [14]. This reagent can block histone 3 citrullination and the formation of NETs, so the Cl-amidine group was used as a positive control group in this experiment [15]. Compared with modern drugs such as Cl-amidine, moxibustion treatment has almost no side effects and is inexpensive, which brings great comfort to the patients; meanwhile, moxibustion is easy to operate, safe, and effective, so it is widely used in the clinic [4].

In this context, this study investigated whether moxibustion improves RA through the NET-NLRP3 inflammasome axis. Specifically, the AA model was established in rats through complete Freund's adjuvant (CFA) injection based on the composite environmental factors including wind, cold, and dampness. Then, moxibustion was applied to Shenshu (BL23) and Zusanli (ST36) acupoints of rats, with Cl-amidine as a positive control.

2. Material and methods

2.1. Animals

Specific pathogen-free Wistar male rats weighing 200 ± 10 g were provided by Liaoning Changsheng Biotechnology Company [SCXK(Liao)2020–0001]. For acclimatization, rats were housed in a laboratory home with a temperature of 21°C–25 °C, relative humidity of 60%–65 %, and a 12 h/12 h light/dark cycle (dark period: 20:00–8:00) for 7 days. The experiments involving animals were conducted under ratification from the Laboratory Animal Ethics Committee of Anhui University of Traditional Chinese Medicine (Ethics No. AHUCM-rats-2022,139) and strictly according to the "Guideline on the Good Treatment of Laboratory Animals" issued by the Ministry of Science and Technology in 2006.

2.2. Main instruments and reagents

The following instruments were used: VE-186 transmembrane and EPS300 electrophoresis instruments (Tennant Company, Shanghai, China), the JW-3021HR high-speed centrifuge (Jiawen Company, Anhui, China), the DHG-9070 electric thermostatic blast drying oven (Sanfa Company, Shanghai, China), the RT-6100 enzyme-linked immunosorbent assay (ELISA) Microplate Reader (Rayto Company, Shenzhen, China), micropipettes (Eppendorf, Hamburg, Germany), the UC-7 ultrathin microtome (Leica, Weztlar, Germany), the JEM1400 transmission electron microscope (Nippon Electron, Tokyo, Japan), the YB-7LF biological tissue embedding machine (Yaguang Company, Hubei, China), and the CX41 microscope (OLYMPUS, Tokyo, Japan).

CFA was purchased from Sigma (St. Louis, Missouri, USA). Uratan, 4 % paraformaldehyde, and polyacrylamide gel electrophoresis (PAGE) gels were acquired from Solarbio (Beijing, China). Cl-amidine was obtained from Selleck (Houston, TX, USA). Glutaraldehyde was provided by TED PELLA (Redding, California, USA). Anhydrous ethanol was acquired from Guangnuo Chemical Technology Co., Ltd. (Shanghai, China). Hematoxylin and eosin (HE) staining solutions were purchased from Xinle Company (Anhui, China). Radio-Immunoprecipitation Assay (RIPA) cell lysis solution (strong) and primary and secondary antibodies for western blotting were obtained from Beyotime (Shanghai, China). The polyvinylidene fluoride membrane was purchased from Millipore (Boston, Massachusetts, USA). The pre-stained protein Marker and electrogenerated chemiluminescence (ECL) ultrasensitive luminescence kit were provided by Thermo Fisher Scientific (Waltham, Massachusetts, USA). Goat anti-mouse and goat anti-rabbit immunoglobulin G and glyceraldehyde-3-phosphate dehydrogenase (GAPDH) antibodies were purchased from Zhongshan JinQiao Company (Beijing, China). Myeloperoxidase (MPO), neutrophil elastase (NE), acyl arginine deiminase 4 (PAD-4), and NLRP3 antibodies were bought from Abcam (Cambridge, UK). Citrullinated histone (Cit-H3) antibodies were acquired from Cell Signaling Technologies (Beverly, Massachusetts, USA). NET antibodies were purchased from Affinity (Texas, USA). The rat interleukin (IL)-1β ELISA kit was bought from Wuhan Genome Company (Hubei, China). The rat anti-cyclic citrullinated peptide antibody (CCP-Ab) ELISA kit was provided by Jianglai Company (Shanghai, China).

2.3. Modeling method

The method of the composite environmental factors, including wind, cold, and dampness, plus CFA injection was used to establish the AA model [16]. All rats, except normal control (NC) rats, were placed in the environment with the above factors for 20 days (the room temperature was maintained at 10 °C, and the cage was sprinkled with water, placed on ice, and blown with a fan directly). On the 21st day, the rats were transferred to a room at 21°C–25 °C, followed by the injection with CFA (0.15 mL/rat) into the right hind toe to stimulate inflammation and establish the AA model. The modeled rats were observed for 3 days. The model was considered to be successfully established when acute inflammatory swelling occurred in the foot and ankle at 24 h and systemic polyarthritis appeared at 48 h, accompanied by redness, swelling, and inflammatory nodules in the right and left forelimbs or lateral limbs, tail, or ears [17]. The rats in the NC group received no treatment and were always maintained at 21°C–25 °C..

2.4. Experimental design (Fig. 1)

The rats were randomly classified into NC and model groups with the random number table method. The successfully modeled rats were further randomly allocated into three groups, including AA, MOX, and Cl-amidine (6 rats for each group).

Treatment of the MOX group After 3 days of model establishment, the bilateral Shenshu (BL23) and Zusanli (ST36) acupoints were positioned as per the atlas of acupoints in Experimental Acupuncture for the suspended moxibustion treatment of AA rats [18]. The selected acupoints of rats acupoints were labeled with color after the hairs on these acupoints were removed. Next, the suspended moxibustion was performed at a distance of 2 cm from the acupoints with special cigarette-type moxa strips (0.7 cm in diameter, Henan Nanyang Huakang Moxa Products Co., Ltd., Henan, China) after rats were fixed on a special suspended wooden frame. Moxibustion was performed for 21 days, 20 min per acupoint (bilateral acupoints were treated simultaneously, and each rat underwent moxibustion by treating two acupoints on the same side every day and the opposite side the next day alternately) and 1 time/day.

Treatment of the Cl-amidine group After 3 days of successful modeling, Cl-amidine was injected intraperitoneally into AA rats with a syringe at a dose of 1 mg/kg/day for 21 days in the absence of moxibustion treatment.

Treatment of the NC or AA group For the NC or AA group, the rats were normally grasped and fixed on a moxibustion frame for the same duration without other treatments.

2.5. Joint swelling degree (JSD) [19] and arthritis index (AI) [20]

The homemade drainage method was used to measure the volume of the right hind footpad below the turning points of the ankle joint on 1 day before treatment and the last day of the experiment, respectively, for calculating the swelling degree of the footpad [21]. The following formula was utilized for calculation: JSD (%) = (Vt-Vn)/Vn × 100 % (Vn and Vt are the footpad volumes before and after the stimulation of inflammation, respectively).

The degree of joint redness, swelling, and deformation of the limbs of rats was observed and recorded on 1 day before treatment and the last day of the experiment, respectively. The AI value of each rat was calculated by summing the scores of 4 limbs using the integration method. The scoring criteria were as follows: no abnormality in joints, 0 points; redness and swelling in the small toe joints, 1 point; swelling in the toe joint and footpad, 2 points; swelling in paw below the ankle joint, 3 points; swelling in the whole foot

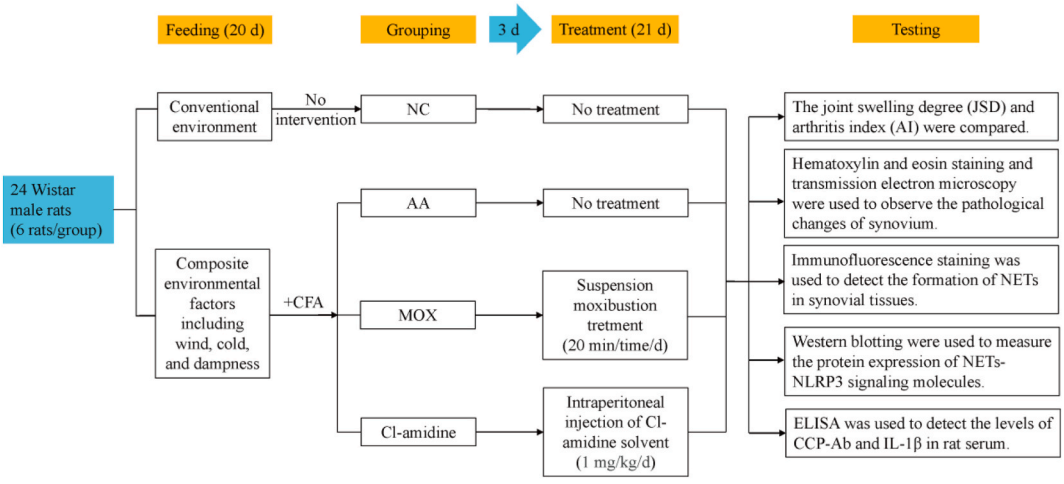

Fig. 1. The pictorial representation of experimental design. After 7 days of adaptive feeding, the rats were randomly classified into NC and model groups with the random number table method. Rats other than NC rats were housed in a combined wind, cold, and dampness environment for 20 days. On the 21st day, the rats were injected with CFA into the right hind toe to establish the AA model. The modeled rats were observed for 3 days. After successful modeling, the rats were randomly divided into AA group, MOX group, and Cl-amidine group, and treated for 21 days each. Tissues were collected 24 h after the last intervention treatment.

including the ankle joint, 4 points.

2.6. HE staining

Three rats were randomly chosen from each group with the random number table method 24 h after the final intervention and anesthetized via the intraperitoneal injection of 20 % uratan solutions (0.6 mL/100 g). The synovial tissues attached beneath the cartilage of the ankle joint were then surgically separated and obtained, followed by 4 % paraformaldehyde fixing, routine dehydration, clearing, and paraffin embedding. Afterward, the tissues were prepared into coronal sections (4–6 μm) for HE and immunofluorescence staining. Paraffin sections were dried in the oven for 30 min at 66 °C, dewaxed in xylene, hydrated in gradient ethanol, stained with hematoxylin for 5 min, and differentiated in 1 % hydrochloric acid alcohol for 30 s, followed by eosin staining for 1 min, gradient ethanol dehydration, xylene clearing, and neutral gum sealing. The results were observed under the microscope and images were acquired.

To quantify the inflammation around the ankle joint in rats, we chose the same location of the ankle joint in different individuals for observation and counted the perisynovial inflammation score [22]. The microscopic view was evaluated.

2.7. Transmission electron microscopy

Three rats were randomly selected from each group 24 h after the final intervention. Synovial tissues were collected from the right hind ankle subsequent to anesthesia and dried on filter paper. A portion of the tissues was used for transmission electron microscopy observation, while the other portion was frozen in liquid nitrogen for western blotting detection. The synovial tissues were immediately subjected to 24-h fixation in 2.5 % glutaraldehyde, 6-h immersion in phosphate-buffered saline (PBS), and 2-h fixation in 1 % osmium acid. The tissues were dehydrated in gradient ethanol, soaked in epoxy resin, embedded for 2 h, and dried in the oven at 45 °C for 12 h and 72 °C for 24 h. Subsequently, the tissues were trimmed and cut into ultra-thin sections (70 nm). The sections were retrieved with copper mesh, stained with uranyl acetate-lead citrate, examined under the transmission electron microscope, and photographed.

2.8. Immunofluorescence staining

Paraffin sections of synovial tissues from rat ankles were prepared and dewaxed, followed by antigen repair with citrate repair solutions. After being permeabilized with 0.5 % Triton X-100 for 30 min, the sections were sealed. The sections were incubated with primary antibodies against NETs (1:200) in an incubator, which was covered, at 37 °C for 1 h and rinsed with PBS, followed by 30-min incubation with immunofluorescent secondary goat anti-rabbit antibodies (1:400) at 37 °C. Next, the sections underwent sealing with anti-fluorescence quenching sealing agents containing 4′,6-Diamidino-2-Phenylindole (DAPI), and the fluorescent sections were scanned with a digital section scanner.

2.9. Western blotting

The frozen synovial tissues (100 mg) were lysed with RIPA solutions and centrifuged at 12,000 r/min for 15 min, followed by total protein extraction from the supernatant. The proteins were subjected to 1 h of sodium dodecyl sulfate-PAGE at a steady pressure of 80 V after being cooled to room temperature and then transferred to the membrane which was sealed for 2 h at room temperature. Thereafter, the membrane was probed with primary antibodies against MPO (1:1000), NE (1:4000), GAPDH (1:2000), Cit-H3 (1:1000), PAD-4 (1:2000), and NLRP3 (1:1000) overnight at 4 °C and then washed with phosphate-buffered saline with Tween 20 (PBST) for 10 min (3 times). The membrane was then incubated with horseradish peroxidase-tagged secondary antibodies (1:20,000) at room temperature for 1.2 h, followed by PBST washing. The ECL luminescence kit was used to calculate the protein concentration. The relative expression of each protein was determined, with GAPDH as the internal reference.

2.10. ELISA

The rats were anesthetized 24 h after the final intervention, and then 5 mL blood was obtained from the abdominal aorta and centrifuged in a freezing centrifuge (a centrifugal radius of 10 cm) at 4 °C and 3000 r/min for 20 min. Afterward, the supernatant was harvested and stored in a refrigerator at −80 °C. The ELISA kits were equilibrated at room temperature for 20 min. The assay was conducted as instructed in the manuals of the kits. After the addition of the termination solution, the optical density (OD) value was measured at 450 nm with the microplate reader, and the standard curve was plotted for calculating the concentrations of CCP-Ab and IL-1β.

2.11. Statistical analysis

The measurement data were summarized as mean ± standard deviation (SD) and were analyzed with SPSS 19.0 software. The data with a normal distribution were compared between groups with the one-way analysis of variance test. Pairwise comparisons between groups were performed with the least significant difference test for data with homogeneity of variance and with Tamhane's T2 for data with heterogeneity of variance. The software GraphPad Prism 7.00 was used to plot images. The difference was considered statistically

significant at $P < 0.05$.

3. Results

3.1. Moxibustion suppressed joint inflammation in AA rats

At the end of the experiment, the efficacy of moxibustion was observed by comparing the limb photographs of adjuvant-treated rats (Fig. 2A–D). As shown in Fig. 2E and F, the JSD and AI scores of rats were assessed. The results revealed that JSD and AI scores were substantially higher in the AA, MOX, and Cl-amidine groups than in the NC group ($P < 0.01$) and statistically insignificantly different among these three groups ($P > 0.05$). After treatment with MOX or Cl-amidine, JSD and AI scores of rats were reduced ($P < 0.01$), and the efficacy of MOX was slightly better than that of Cl-amidine. In addition, ACPA and cytokine concentrations responded to the overall inflammation level in RA. Moxibustion treatment significantly decreased the expression of CCP-Ab (Fig. 3A) and IL-1β (Fig. 3B) in the serum of AA rats ($P < 0.01$).

3.2. Moxibustion attenuated synovial pathological injury in AA rats

HE staining was conducted to assess the pathological changes of rat ankle synovial tissues (Fig. 4A–D). The results demonstrated that rats in the NC group had smooth ankle synovial membranes and a small amount of inflammatory cell infiltration, without hyperplasia. In comparison to those in the NC group, rats in the AA group displayed a larger amount of inflammatory cell infiltration and hyperplasia. Furthermore, moxibustion and Cl-amidine suppressed the invasion of inflammatory cells. In addition, peri-synovial inflammation in the rat ankle joint was quantitatively assessed based on sections (Fig. 4E). The inflammation score showed significantly elevated inflammation in the AA group compared to the NC group ($P < 0.01$), whereas the inflammation was alleviated in both the MOX and Cl-amidine groups after treatment ($P < 0.01$).

The ultrastructural alterations of synovial cells were observed with transmission electron microscopy. In the NC group (Fig. 5A), synovial cells showed smooth and intact nuclear membranes, distinct mitochondrial boundaries, and visible cristae. The nuclear membrane of synovial cells was incomplete and hazy in the AA group (Fig. 5B), with an irregular shape, murky mitochondrial membrane boundaries, evident swelling, and disrupted cristae. The nuclear membrane of synovial cells was smooth and clear in the MOX group (Fig. 5C), with no obvious enlargement of the mitochondria, still visible cristae, and distinct membrane boundaries. The mitochondria of synovial cells were slightly swollen and the cristae were visible in rats of the Cl-amidine group (Fig. 5D), accompanied by clear nuclear membranes. Accordingly, in contrast to the NC group, the synovial cells of rats in the AA group had significant pathological changes. Moreover, both moxibustion and Cl-amidine ameliorated synovial cell damage to varying degrees, among which

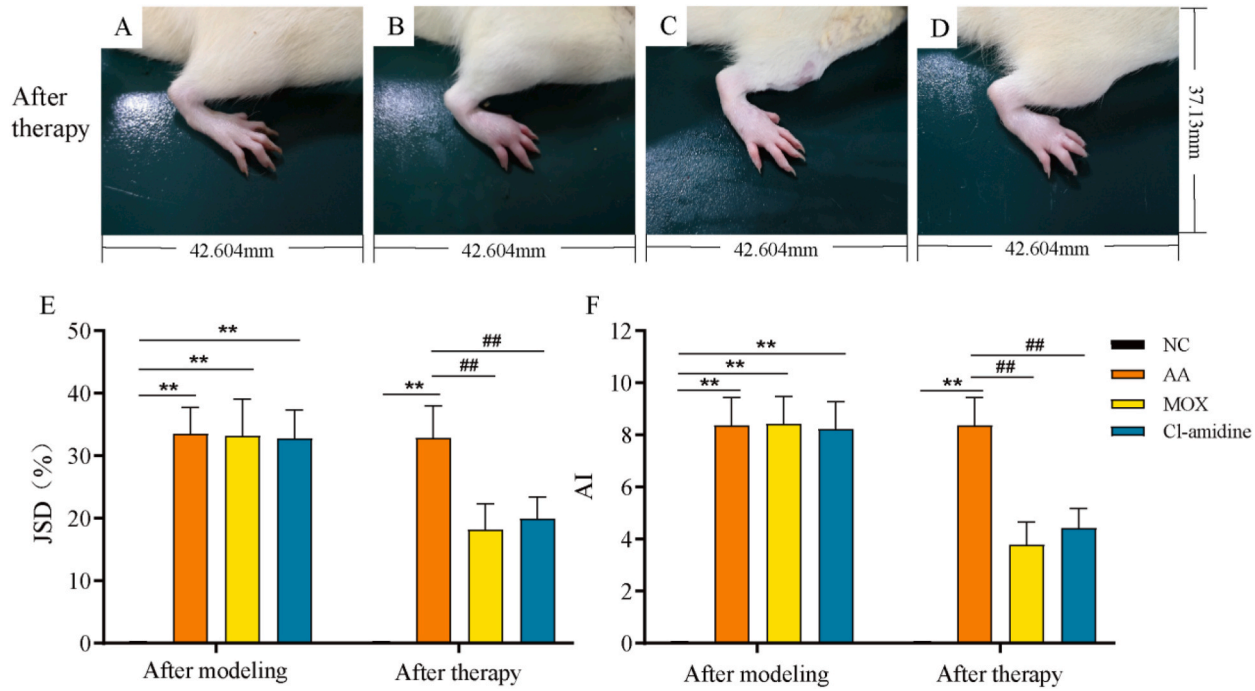

Fig. 2. Morphological observation of rats. A-D. The typical image of the right hind footpad of rats after the therapy. A: the NC group, B: the AA group, C: the MOX group, D: the Cl-amidine group. **E.** JSD score of rats. **F.** AI scores of rats. n = 6 rats/group. Data were expressed as mean ± standard deviation. $^{**}P < 0.01$ compared to the NC group at the same time. $^{\#\#}P < 0.01$ compared to the AA group at the same time.

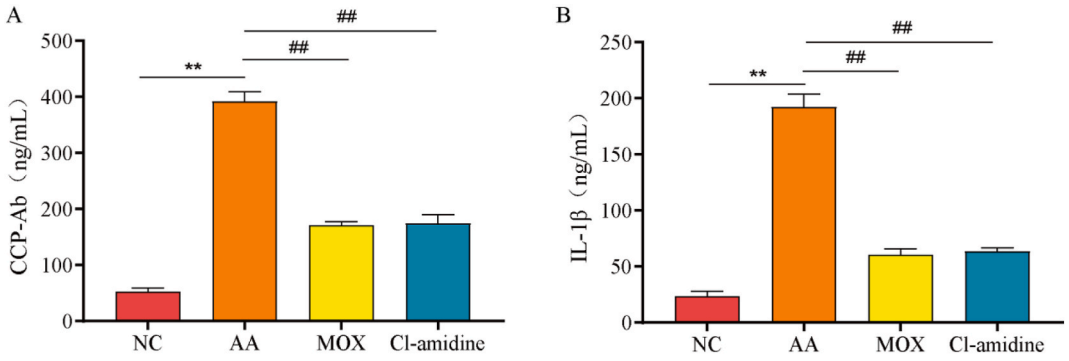

Fig. 3. Moxibustion inhibits the secretion of ACPA and IL-1β. A. The quantity of CCP-Ab in the serum of rats. **B**. The amount of IL-1β in the serum of rats. n = 6 rats/group. The results were summarized as mean ± standard deviation. $^{**}P < 0.01$ compared to the NC group. $^{\#\#}P < 0.01$ compared to the AA group.

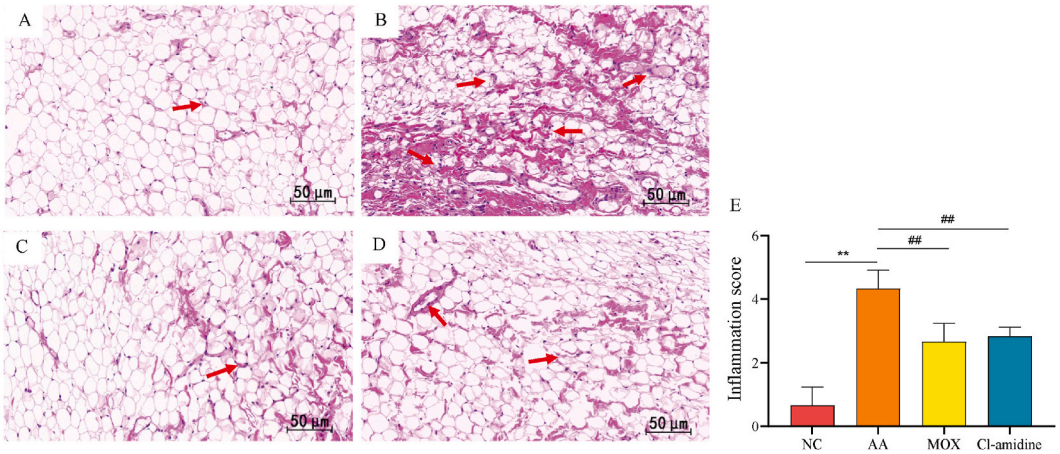

Fig. 4. Histological assessment of the rat ankle synovium. A-D. HE staining was performed for analyzing histological changes in the rat ankle synovium of the NC (A), AA (B), MOX (C), and Cl-amidine (D) groups. Red arrows indicate inflammatory cell infiltration. 20 × . **E.** Inflammation was scored in HE-stained sections. n = 3 rats/group. Data were expressed as mean ± standard deviation. $^{**}P < 0.01$ compared to the NC group. $^{\#\#}P < 0.01$ compared to the AA group.

MOX marginally outperformed Cl-amidine.

3.3. Moxibustion repressed the formation of NETs in the synovial tissues of AA rats

The formation of NETs in rat synovial tissues was analyzed with immunofluorescence staining. In the fluorescence sections (Fig. 6A–D), little NETs were formed in the NC group, without an obvious structure. The AA group displayed a large number of fibrous network-like structures of NETs and a significant increase in NET formation, whilst the MOX and Cl-amidine groups had fewer NET structures. Then, NETs were quantitatively analyzed (Fig. 6E), which exhibited that the OD value of NETs in rat synovial tissues was higher in the AA group than in the NC group ($P < 0.01$), whereas moxibustion and Cl-amidine reduced the number of NETs ($P < 0.01$).

3.4. Moxibustion downregulated the expression of NET-related components and NLRP3 in AA rats

The expression of NET production-related factors (MPO, NE, Cit-H3, and PAD-4) and the key inflammasome marker (NLRP3) was detected and quantified with western blotting to probe the anti-inflammatory mechanism of moxibustion (Fig. 7A, refer to the supplementary document for the complete images). The results indicated elevations in the expression of MPO, NE, Cit-H3, PAD-4, and NLRP3 in rat synovial membranes after AA modeling ($P < 0.01$). Moxibustion positively diminished the expression of NET components and NLRP3, with similar effects to Cl-amidine ($P < 0.01$) (Fig. 7B–F).

4. Discussion

In traditional Chinese medicine, RA is defined as an “arthralgia syndrome” [23]. Moreover, ancient physicians believed that RA

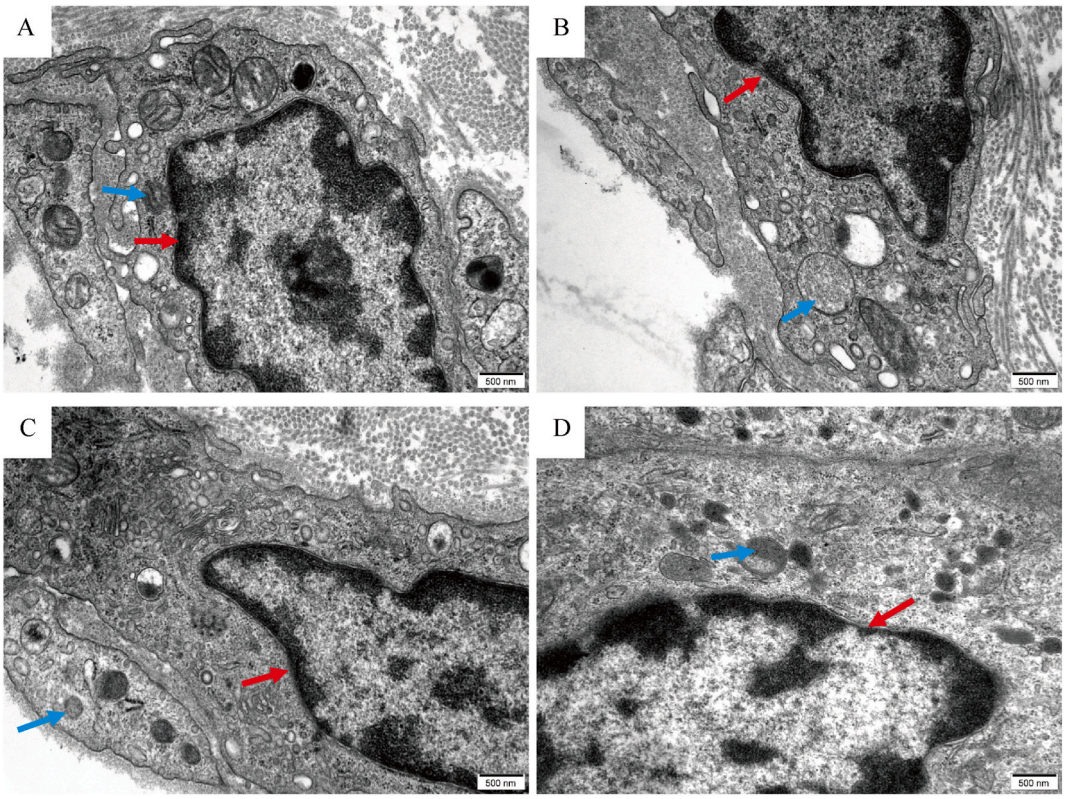

Fig. 5. The ultrastructure of rat ankle synovial cells. A-D. Transmission electron microscopy was performed to observe representative images of rat ankle synovial cells in the NC group (A), the AA group (B), the MOX group (C), and the Cl-amidine group (D). Red arrows represent nuclei, and blue arrows mark mitochondria. Magnification: 30,000×.

occurrence is associated with innate debility, deficiency of vital qi, weakened defensive qi, and simultaneous exposure to wind, cold, dampness, heat, phlegm, and stasis. In modern medicine, the occurrence of RA has been believed to be attributed to spleen qi deficiency, liver-kidney deficiency, and attack by exogenous pathogenic elements [24,25]. Moxibustion is made of moxa floss, which is an important part of traditional Chinese medicine, and when lit, it stimulates the body's acupoints with warmth and heat so as to achieve the purpose of warming Yang for dispelling cold, supporting Yang to remove paralysis, dispelling dampness, and relieving pain [26]. In this study, we ascertained the alleviatory mechanism of moxibustion in the treatment of RA. Specifically, the Shenshu (BL23) and Zusanli (ST36) acupoints were chosen for interventional treatment. As reported, moxibustion on the Shenshu (BL23) acupoint can warm Yang, tonify the kidney, and mobilize the vital qi of the human body. Additionally, moxibustion on the Zusanli (ST36) acupoint can invigorate the spleen, benefit the stomach, and strengthen and consolidate body resistance. Moxibustion on the two acupoints can tonify the innate and acquired essence to maintain the body in a balanced state of yin and yang.

RA is typically characterized by synovial inflammation and hyperplasia, whose occurrence is associated with immune system disorder-induced antibody production and inflammatory factor secretion [27]. CCP-Ab is a member of the ACPA family that is highly specific for the diagnosis of RA, and IL-1β is a key pro-inflammatory factor, both of which can be used as pivotal serological indicators to predict disease development [28]. The ELISA results in our study unveiled that the serum levels of CCP-Ab and IL-1β in the AA group were higher than those in the NC group ($P < 0.01$), indicating that inflammation was substantially promoted in the AA rat model. Furthermore, CCP-Ab and IL-1β levels were significantly reduced by treatment with MOX or Cl-amidine ($P < 0.01$), with the effect of MOX superior to that of Cl-amidine. This result illustrated that inflammation was suppressed in AA rats by these intervention treatments. We also found that moxibustion reduced the JSD and AI pathology scores of rats ($P < 0.01$), showing the improvement of arthritis symptoms by moxibustion. By HE staining, the synovial inflammatory cell infiltration was significantly increased in the modeled rats compared to the NC group, which was alleviated after the intervention; similarly, transmission electron microscopy confirmed that moxibustion inhibited synovitis injury in AA rats. The improvement of joint inflammation corresponded to the decrease in the serum levels of CCP-Ab and IL-1β. All of these findings confirmed the effectiveness of moxibustion in attenuating inflammation in RA.

Inflammasomes are thought to play a critical role in host defense against invading pathogens as well as in the development of spontaneous inflammatory diseases, and NLRP3 inflammasome is currently the most characterized and can be expressed in peripheral monocytes, macrophages, central microglia, and dendritic cells [29,30]. The progression of RA depends on the activation of NLRP3 inflammasome and the release of the pro-inflammatory cytokine IL-1β [31]. Prior research unraveled that NLRP3 inhibition or

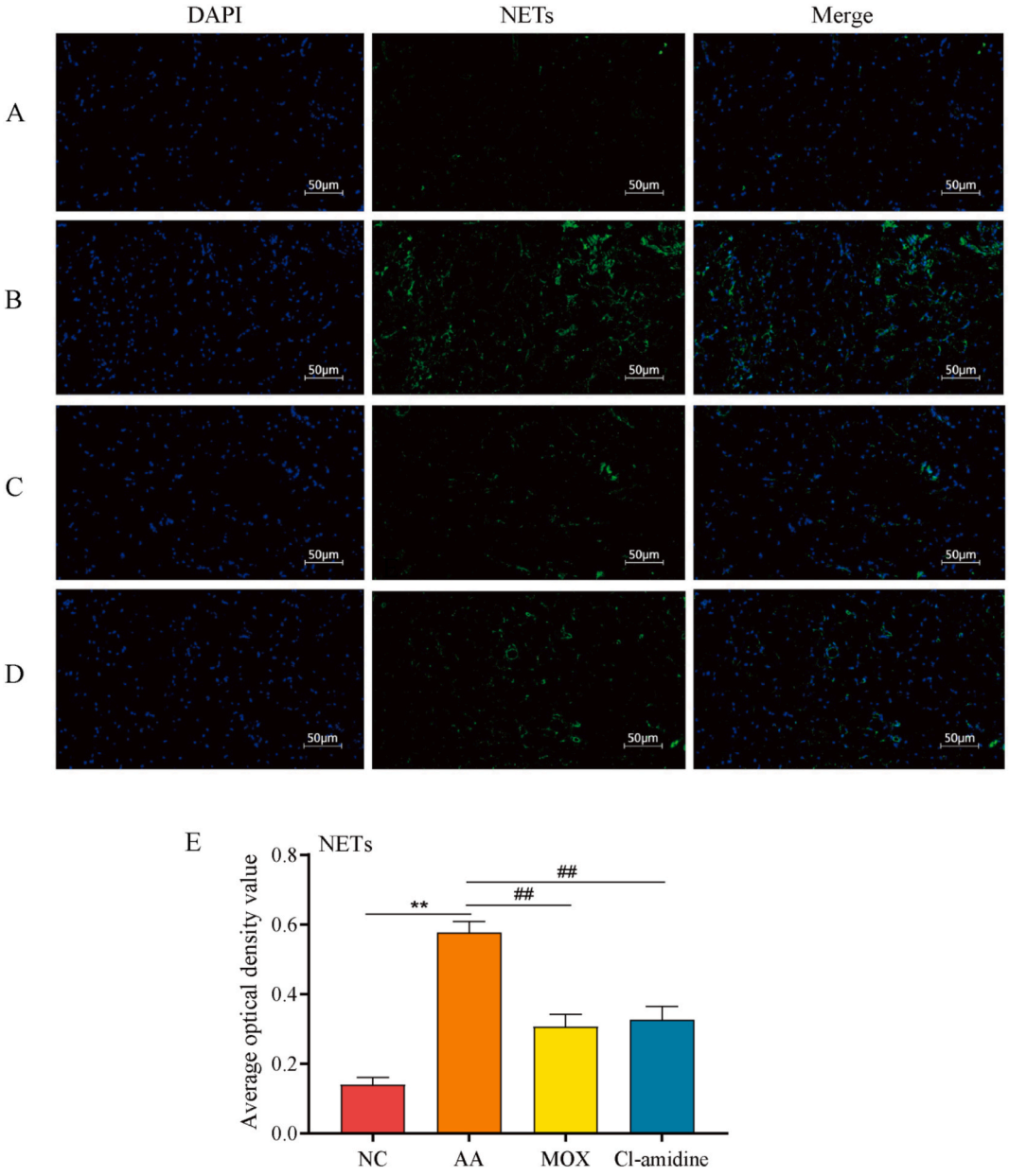

Fig. 6. Moxibustion depresses the formation of NETs in rat synovial tissues. Immunofluorescence staining was performed with DAPI (blue) and anti-NET antibody (green) and observed under the confocal microscope. **A-D**. The nuclei are blue in color and the location of NETs positive expression is green. A: the NC group, B: the AA group, C: the MOX group, D: the Cl-amidine group. NETs formed in rats after AA modeling, which was neutralized by MOX and Cl-amidine. Compared with the NC group, the fluorescence intensity of NETs was significantly higher after adjuvant intervention; compared with the AA group, the fluorescence intensity of NETs was markedly lower in both the MOX and Cl-amidine groups. **E.** A quantitative analysis of NETs was performed, which revealed that MOX decreased the optical density value of NETs, similar to the effect of Cl-amidine. n = 3 rats/group. Data were expressed as mean ± standard deviation. $^{**}P < 0.01$ compared to the NC group. $^{\#\#}P < 0.01$ compared to the AA group.

knockdown greatly decreased joint inflammation and bone deterioration in RA models, indicating NLRP3 activation as a prerequisite for NLRP3 inflammasome assembly [32,33]. Our study showed that NLRP3 protein levels were reduced in synovial tissues of AA rats after moxibustion intervention ($P < 0.01$), suggesting an inhibitory effect of moxibustion on inflammasome expression, consistent with earlier findings [34]. In addition, NETs, an essential source of autoantigens, mediate tissue damage in many experimental models of autoimmune disorders (such as RA and systemic lupus erythematosus), and their components are considered danger-associated molecular patterns (DAMPs) that activate NLRP3 inflammasome, break self-tolerance, facilitate inflammatory factor secretion, and accelerate autoimmune responses [35,36]. Given the fact that NLRP3 inflammasome is regulated by NETs, it is reasonably hypothesized that the inhibition of NLRP3 inflammasome assembly by moxibustion suppresses inflammation in AA rats by involving the

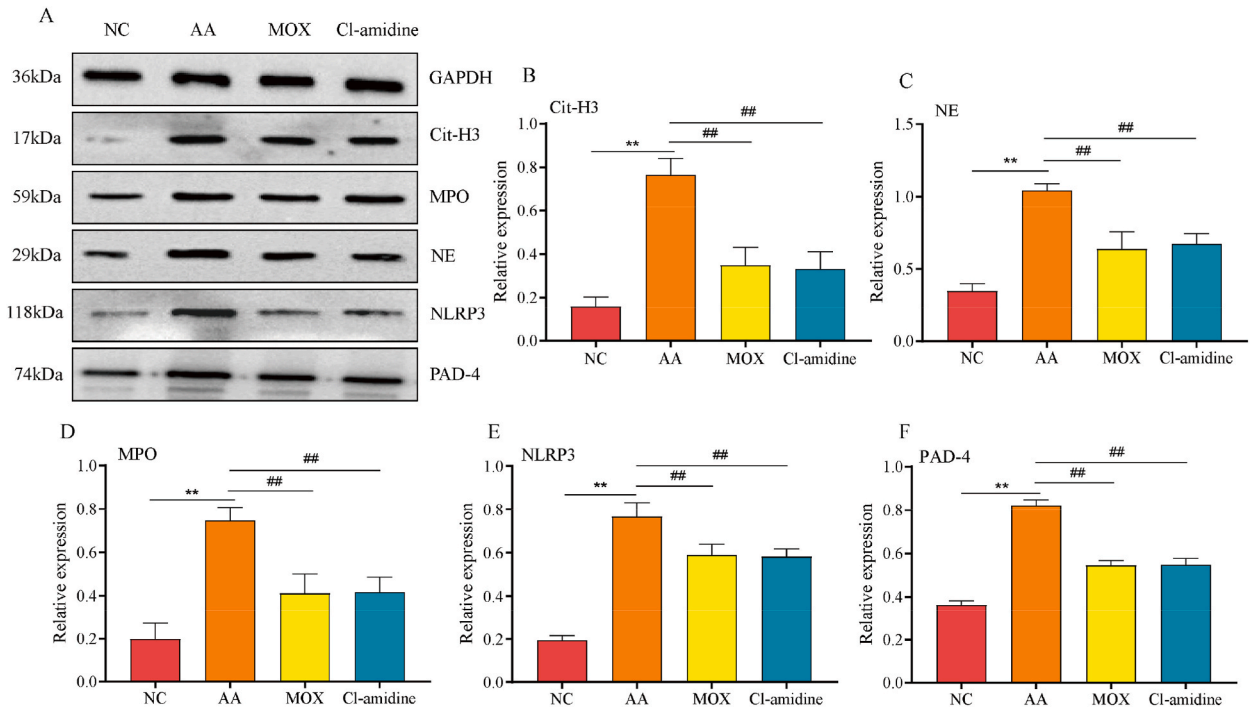

Fig. 7. Moxibustion lowers the protein levels of NET-related components and NLRP3. A. Western blotting results of NET-related proteins and NLRP3 in the synovial membrane of rats (Refer to the supplementary document for the complete images). **B–F**. Quantitative results of expression of each protein in (A). n = 3 rats/group. The results were expressed as mean ± standard deviation. $^{**}P < 0.01$ compared to the NC group. $^{\#\#}P < 0.01$ compared to the AA group.

regulatory role of NETs.

In the early stages of RA, neutrophils are activated and recruited into the joint cavity, thus secreting numerous cytokines and then maintaining the local inflammatory state [37]. Neutrophils also defend against pathogenic microbial invasion through the formation of NETs [38]. In autoimmune diseases, the imbalance between the formation and clearance of NETs results in the deposition of excess NETs in tissues and organs, which promotes inflammation and drives disease progression [12]. In RA, NETs produce citrulline neoepitopes that can contribute to the loss of immunological tolerance and the generation of ACPAs and cytokines [39]. Therefore, the synthesis of aberrant NETs is a key factor in the pathogenesis of RA, and NETs may be a major therapeutic target for RA.

NET components are a chromatin fibrillar meshwork released extracellularly by neutrophils that are activated and stimulated by multiple factors, in which double-stranded DNA is the backbone and is interspersed with protein molecules, such as Cit-H3, MPO, NE, and PAD-4 [39]. During the formation of NETs, MPO is a local mediator of joint damage and NE is linked to cartilage destruction in RA. Together, these two factors synergistically drive chromatin depolymerization. PAD-4, a key enzyme, can catalyze histone citrullination and participate in the formation of Cit-H3. Prior studies revealed that Cl-amidine, the most potent chemical inhibitor of PAD-4, affected the immune system by blocking NET formation and reduced disease severity in a mouse model of RA-related joint injury in a dose-dependent manner [40,41]. Therefore, Cl-amidine was utilized as a positive control in our research to verify whether moxibustion can exert a repressive effect on inflammation in RA by affecting the formation of NETs. Specifically, our immunofluorescence assay exhibited that the formation of NETs markedly increased in rat synovial tissues subsequent to AA modeling ($P < 0.01$) and declined in AA rats after interventions with MOX or Cl-amidine ($P < 0.01$). Therefore, moxibustion may mitigate RA by inhibiting the formation of NETs, similar to the effect of the NET formation inhibitors. Western blotting findings suggested that overproduction of NETs and high activation of NLRP3 inflammasome were evident in the synovial membrane of rats after AA modeling, as evidenced by a marked enhancement in the protein expression of NET-related components (MPO, NE, Cit-H3, and PAD-4) and the essential component of the inflammasome NLRP3 in the synovial tissues ($P < 0.01$). Conversely, the protein expression of MPO, NE, Cit-H3, PAD-4, and NLRP3 was diminished by treatments ($P < 0.01$), also confirming that moxibustion might reduce the expression of NETs and related components to alleviate synovial inflammatory damage in RA. Consistently, a prior study exhibited that andrographolide exerted alleviatory effects on RA by preventing the synthesis of NETs and the release of their constituents [42]. There are also researchers who have found through in vivo and in vitro experiments that Tetrandrine, which is derived from traditional Chinese medicine, not only reduces the degree of pathological damage in RA but also produces a favorable therapeutic effect on RA by modulating the inflammation and NET formation in which neutrophils are involved [43].

Abnormal expression of NETs triggers inflammation, which in Chinese medicine theory is caused by an imbalance of yin and yang in the body, poor qi and blood circulation, and invasion of evil qi, etc. Treating inflammation by regulating the balance of yin and yang and activating blood circulation through moxibustion therapy in Chinese medicine is one of the effective methods for restoring the

health of the organism. In this study, we found that the efficacy of moxibustion therapy was comparable to the inhibition of NETs through observation. The trend of NETs-related indexes after moxibustion indicated that moxibustion could play a role in down-regulating the expression of NETs in the body and inhibiting their production, thus improving arthritis symptoms.

5. Conclusion

In summary, our findings demonstrated that moxibustion on the Shenshu (BL23) and Zusanli (ST36) acupoints substantially ameliorated the synovitis symptoms in AA rats potentially by repressing the production of NETs, the expression of their related proteins, and the activation of NLRP3 inflammasome, all of which repressed inflammation and lower the release of the inflammatory cytokine IL-1β. NETs are effective targets for the treatment of RA. Nevertheless, there are still some limitations in this experiment, because of the lack of funds and experimental conditions, the sample size for tissue analysis is small. Little is known regarding the mechanisms by which different stimuli lead to the formation of different NETs and the pathways through which moxibustion acts on NETs, which calls for further investigation. In conclusion, our results illustrated that moxibustion is an effective strategy for the treatment of RA.

Funding

This study was supported by the National Natural Science Foundation of China (No. 81403484); Anhui Province University Natural Science Fund Project of China (No. KJ2019A0448); National Project Cultivation Fund Project Plan (No. 2019py01); Anhui Province Clinical Medical Research Center [Anhui Provincial Science and Technology Department Anhui Social Science (2020) No. 41]; Anhui Province Traditional Chinese Medicine Inheritance Innovation Scientific Research Project (No. 2020ccyb13); The training Program of Outstanding talents in Colleges and Universities (No. gxgnfx2021122); Anhui Province Medical and Health Key Specialist Construction Project (Anhui Health Letter [2021] No. 273); Project of Anhui Provincial Department of Education (No. 2023AH050858); Project of Outstanding Talents in Health and Wellness [(2022) No. 392].

Data availability statement

Data will be made available on request.

CRediT authorship contribution statement

Miao Wang: Writing – original draft. **Hongfang Zhao:** Investigation. **Hui Zhao:** Investigation. **Chenlu Huo:** Investigation. **Yu Yuan:** Investigation. **Yan Zhu:** Supervision, Project administration.

Declaration of competing interest

The authors declare that they have no known competing financial interests or personal relationships that could have appeared to influence the work reported in this paper.

Acknowledgment

Thanks to Anhui University of Chinese Medicine for providing the research platform for the experiment.

Appendix A. Supplementary data

Supplementary data to this article can be found online at https://doi.org/10.1016/j.heliyon.2023.e23633.

References

[1] A.F. Radu, S.G. Bungau, Management of rheumatoid arthritis: an overview, Cells 10 (11) (2021) 2857, https://doi.org/10.3390/cells10112857.
[2] C.M. Weyand, J.J. Goronzy, The immunology of rheumatoid arthritis, Nat. Immunol. 22 (1) (2021) 10–18, https://doi.org/10.1038/s41590-020-00816-x.
[3] Y. Sun, J. Liu, L. Xin, et al., Xinfeng capsule inhibits inflammation and oxidative stress in rheumatoid arthritis by up-regulating linc 00638 and activating nrf 2/ho-1 pathway,J. Ethnopharmacol. 3012022) 115839, https://doi.org/10.1016/j.jep.2022.115839..
[4] C. Liao, S. Tao, Y. Xiong, et al., The effects and potential mechanisms of moxibustion for rheumatoid arthritis-related pain: a randomized, controlled trial, J. Pain Res. 162023) 1739-1749, https://doi.org/10.2147/JPR.S408814..
[5] Q. Zhou, H.W. Yu, Y. Zhu, et al., Effects of spleen and kidney acupuncture on inflammatory factors and cartilage matrix in adjuvant arthritis rats, Zhongguo Zhen Jiu 42 (6) (2022) 641–646, https://doi.org/10.13703/j.0255-2930.20210419-0004.
[6] Y. Zhu, H.W. Yu, Y.Z. Pan, et al., Effect of moxibustion at "zusanli"(st36) and "shenshu"(bl23) on mir-155-mediated tlr4/nf-κb signaling involving amelioration of synovitis in rheumatoid arthritis rats, Zhen Ci Yan Jiu 46 (3) (2021) 194–200, https://doi.org/10.13702/j.1000-0607.200377.
[7] Y. Wang, S. Tao, Z. Yu, et al., Effect of moxibustion on beta-ep and dyn levels of pain-related indicators in patients with rheumatoid arthritis, Evid.-based Complement Altern. Med. 20212021) 6637554, https://doi.org/10.1155/2021/6637554..

[8] M. Wang, Y. Zhu, H. Zhao, H.F. Zhao, Exploring the efficacy mechanism of moxibustion to improve synovitis in rats with adjuvant arthritis based on nlrp3/caspase-1/il-1β signaling pathway, Zhen Ci Yan Jiu, https://doi.org/10.13702/j.1000-0607.20220801..
[9] H.U. Scherer, T. Haupl, G.R. Burmester, The etiology of rheumatoid arthritis, J. Autoimmun. 1102020) 102400, https://doi.org/10.1016/j.jaut.2019.102400..
[10] C.Y. Wu, H.Y. Yang, J.H. Lai, Anti-citrullinated protein antibodies in patients with rheumatoid arthritis: biological effects and mechanisms of immunopathogenesis, Int. J. Mol. Sci. 21 (11) (2020), https://doi.org/10.3390/ijms21114015.
[11] R. Khandpur, C. Carmona-Rivera, A. Vivekanandan-Giri, et al., Nets are a source of citrullinated autoantigens and stimulate inflammatory responses in rheumatoid arthritis, Sci. Transl. Med. 5 (178) (2013), https://doi.org/10.1126/scitranslmed.3005580, 178ra40.
[12] E. Fousert, R. Toes, J. Desai, Neutrophil extracellular traps (nets) take the central stage in driving autoimmune responses, Cells 9 (4) (2020) 915, https://doi.org/10.3390/cells9040915.
[13] C. Wang, J. Wang, X. Liu, et al., Cl-amidine attenuates lipopolysaccharide-induced mouse mastitis by inhibiting nf-kappab, mapk, nlrp3 signaling pathway and neutrophils extracellular traps release, Microb. Pathog. 1492020) 104530, https://doi.org/10.1016/j.micpath.2020.104530..
[14] J.M. Adrover, S. Mcdowell, X.Y. He, D.F. Quail, M. Egeblad, Networking with cancer: the bidirectional interplay between cancer and neutrophil extracellular traps, Cancer Cell 41 (3) (2023) 505–526, https://doi.org/10.1016/j.ccell.2023.02.001.
[15] M. Suzuki, J. Ikari, R. Anazawa, et al., Pad 4 deficiency improves bleomycin-induced neutrophil extracellular traps and fibrosis in mouse lung, Am. J. Respir. Cell Mol. Biol. 63 (6) (2020) 806–818, https://doi.org/10.1165/rcmb.2019-0433OC.
[16] C.Y. Peng, L. Hu, Z.J. Wu, J. Wang, R.L. Cai, Effect of moxibustion on the regulation of iron death-related factors in the synovial tissue of knee joints of rats with adjuvant arthritis, Zhen Ci Yan Jiu 47 (1) (2022) 21–26, https://doi.org/10.13702/j.1000-0607.20210837.
[17] Y.C. Ma, F. Duan, M. Meng, X.Y. Guo, S.R. Kou, Y.M. Ma, Preparation of rheumatoid arthritis model in rats with modified freund's complete adjuvant, Xian Dai Yu Fang. Yi Xue (10) (2008) 1989–1991.
[18] S.G. Yu, B. Xu, Experimental Acupuncture and Moxibustion, Tuina and Acupuncture, third ed., Ren Min Wei Sheng Chu Ban She, Beijing, 2021, p. 298.
[19] W. Wei, X.M. Wu, Y.J. Li, Pharmacological Experimental Methodology, Ren Min Wei Sheng Chu Ban She, Beijing, 2010, p. 1722.
[20] L.J. Yan, S.Q. Tong, J. Liu, D.M. Gao, N.F. Chen, J. Hu, Therapeutic effects and mechanisms of tlr4/nf-κb signaling pathway mediated by total peony glycosides in rheumatoid arthritis model rats, Jilin Da Xue Xue Ban (Yi Xue Ban) 47 (2) (2021) 390–396, https://doi.org/10.13481/j.1671-587x.20210219.
[21] Y. Zhu, M. Zhang, C. Zhao, Effects of moxibustion on the intestinal flora of rats with adjuvant arthritis, Zhongguo Zhen Jiu 41 (10) (2021) 1119–1125, https://doi.org/10.13703/j.0255-2930.20201010-k0003.
[22] Y. Zhou, X. Yang, J. Liu, M. Yang, C. Ye, L. Zhu, Carboxyamidotriazole alleviates pannus formation and cartilage erosion in rats with adjuvant arthritis, Heliyon 9 (9) (2023), e20105, https://doi.org/10.1016/j.heliyon.2023.e20105.
[23] Z.M. Zheng, J.C. Chen, M.S. Qiu, Exploring the current status and problems of research on rheumatoid arthritis and Chinese medical evidence, Feng Shi Bing Yu Guan Jie Yan 9 (1) (2020) 54–56, https://doi.org/10.3969/j.issn.2095-4174.2020.01.017.
[24] H.L. Ma, Z.W. Zhao, L.H. Huang, Y.P. Li, Exploring the theory of rheumatoid arthritis treatment from the spleen and kidney, Feng Shi Bing Yu Guan Jie Yan 11 (6) (2022) 57–59, https://doi.org/10.3969/j.issn.2095-4174.2022.06.015.
[25] H. Zhou, Y. Zhong, X. Gao, F. Wu, M. Jia, X. Yang, Efficacy of moxa-burning heat stimulating zusanli(st36) and shenshu(bl23) on expressions of macrophage migration inhibitory factor and macrophage apoptosis in rabbits with adjuvant-induced arthritis, J. Tradit. Chin. Med. 42 (6) (2022) 980–987.
[26] M. Zhang, C. Zhao, L. Jiang, Y. Zhu, Clinical efficacy and mechanism of moxibustion combined with western medicine in the treatment of rheumatoid arthritis with liver and kidney deficiency, Zhongguo Zhen Jiu 41 (5) (2021) 489–492, https://doi.org/10.13703/j.0255-2930.20200519-k0005.
[27] C.Y. Wu, H.Y. Yang, S.F. Luo, J.H. Lai, From rheumatoid factor to anti-citrullinated protein antibodies and anti-carbamylated protein antibodies for diagnosis and prognosis prediction in patients with rheumatoid arthritis, Int. J. Mol. Sci. 22 (2) (2021), https://doi.org/10.3390/ijms22020686.
[28] X. Dong, Z. Zheng, P. Lin, et al., Acpas promote il-1beta production in rheumatoid arthritis by activating the nlrp3 inflammasome, Cell. Mol. Immunol. 17 (3) (2020) 261–271, https://doi.org/10.1038/s41423-019-0201-9.
[29] S.M. Man, T.D. Kanneganti, Regulation of inflammasome activation, Immunol. Rev. 265 (1) (2015) 6–21, https://doi.org/10.1111/imr.12296.
[30] Z. Li, J. Guo, L. Bi, Role of the nlrp3 inflammasome in autoimmune diseases, Biomed. Pharmacother. 1302020) 110542, https://doi.org/10.1016/j.biopha.2020.110542..
[31] F.L. van de Veerdonk, M.G. Netea, C.A. Dinarello, L.A.B. Joosten, Inflammasome activation and il-1beta and il-18 processing during infection, Trends Immunol. 32 (3) (2011) 110–116, https://doi.org/10.1016/j.it.2011.01.003.
[32] X. Yang, N. Zhan, Y. Jin, et al., Tofacitinib restores the balance of γδtreg/γδt17 cells in rheumatoid arthritis by inhibiting the nlrp3 inflammasome, Theranostics 11 (3) (2021) 1446–1457, https://doi.org/10.7150/thno.47860.
[33] C. Guo, R. Fu, S. Wang, et al., Nlrp3 inflammasome activation contributes to the pathogenesis of rheumatoid arthritis, Clin. Exp. Immunol. 194 (2) (2018) 231–243, https://doi.org/10.1111/cei.13167.
[34] J. Chen, H.H. Liu, X.Q. Lu, et al., Effects of moxibustion on the levels of nlrp3 inflammatory vesicle activators cathepsin-b and ros in synovial tissue of rabbits with experimental rheumatoid arthritis, Zhong Hua Zhong Yi Yao Xue Kan 40 (9) (2022) 152–157, https://doi.org/10.13193/j.issn.1673-7717.2022.09.034.
[35] A. Bonaventura, A. Vecchie, A. Abbate, F. Montecucco, Neutrophil extracellular traps and cardiovascular diseases: an update, Cells 9 (1) (2020), https://doi.org/10.3390/cells9010231.
[36] S.K. Jorch, P. Kubes, An emerging role for neutrophil extracellular traps in noninfectious disease, Nat. Med. 23 (3) (2017) 279–287, https://doi.org/10.1038/nm.4294.
[37] C. Carmona-Rivera, P.M. Carlucci, E. Moore, et al., Synovial fibroblast-neutrophil interactions promote pathogenic adaptive immunity in rheumatoid arthritis, Sci. Immunol. 2 (10) (2017), https://doi.org/10.1126/sciimmunol.aag3358.
[38] A.L. Rios-Lopez, G.M. Gonzalez, R. Hernandez-Bello, A. Sanchez-Gonzalez, Avoiding the trap: mechanisms developed by pathogens to escape neutrophil extracellular traps, Microbiol. Res. 2432021) 126644, https://doi.org/10.1016/j.micres.2020.126644..
[39] G. Wigerblad, M.J. Kaplan, Neutrophil extracellular traps in systemic autoimmune and autoinflammatory diseases, Nat. Rev. Immunol. (2022) 1–15, https://doi.org/10.1038/s41577-022-00787-0.
[40] A.H. Schneider, C.C. Machado, F.P. Veras, et al., Neutrophil extracellular traps mediate joint hyperalgesia induced by immune inflammation, Rheumatology 60 (7) (2021) 3461–3473, https://doi.org/10.1093/rheumatology/keaa794.
[41] S. Mondal, P.R. Thompson, Protein arginine deiminases (pads): biochemistry and chemical biology of protein citrullination, Accounts Chem. Res. 52 (3) (2019) 818–832, https://doi.org/10.1021/acs.accounts.9b00024.
[42] X.H. Li, Study on the Mechanism of Andrographis Paniculata Lactone in the Treatment of Rheumatoid Arthritis by Modulating Neutrophil Activity, Beijing Zhong Yi Yao Da Xue, 2020, https://doi.org/10.26973/d.cnki.gbjzu.2020.000793.
[43] Q. Lu, H. Jiang, Q. Zhu, et al., Tetrandrine ameliorates rheumatoid arthritis in mice by alleviating neutrophil activities, Evid.-based Complement Altern. Med. 20222022) 8589121, https://doi.org/10.1155/2022/8589121..